ELSEVIER

Journal of Molecular Catalysis A: Chemical 149 (1999) 225–232

JOURNAL OF MOLECULAR CATALYSIS A: CHEMICAL

www.elsevier.com/locate/molcata

Highly dispersed cobalt in $CuCo/SiO_2$ cluster-derived catalyst

Jordi Llorca [a], Narcís Homs [a,*], Oriol Rossell [a], Miquel Seco [a], José-Luis G. Fierro [b], Pilar Ramírez de la Piscina [a,1]

[a] *Departament de Química Inorgànica, Facultat de Química, Universitat de Barcelona, Diagonal 647, 08028 Barcelona, Spain*
[b] *Instituto de Catálisis y Petroleoquímica, CSIC, Campus UAM, Cantoblanco, 28049 Madrid, Spain*

Received 1 January 1999; received in revised form 5 March 1999; accepted 5 March 1999

Abstract

A silica-supported CuCo catalyst has been prepared by anchoring a Cu–Co bimetallic complex. Evolution of the species under vacuum and CO treatments has been followed by in situ FTIR. A breakdown of the initial complex with CO at 373 K gives $[Co(CO)_4]^-$. After total decarbonylation, a subsequent CO treatment followed by FTIR indicates the presence of metallic Cu and very small particles of cobalt. The catalyst obtained after an H_2-treatment at 473 K has been characterized by XRD, TEM and XPS techniques. The presence of large Cu particles and highly-dispersed subnanometric cobalt particles is inferred. Coordination of CO on these very small particles of metallic cobalt could give $Co_4(CO)_{12}$. Catalytic behaviour in the hydroformylation of ethylene and in the hydrogenation of CO is related to the highly dispersed cobalt, which probably interacts with Cu. An easy CO insertion into a metal–alkyl bond is favoured over this CuCo catalyst.

Keywords: Bimetallic catalyst; Copper–cobalt catalysts; Higher alcohol synthesis; Cluster-derived catalysts

1. Introduction

Clusters or metal complexes can be used as precursors to prepare metal-supported catalysts. After the interaction of metal complexes with the support surface, the removal of ligands can frequently be carried out under mild hydrogen treatment. This method of preparation is particularly interesting when low valence state metal complexes are used and ligand removal is easy [1,2]. Moreover, the preparation of supported bimetallic catalysts from bimetallic complexes may lead to catalysts with new characteristics, where a specific interaction between the two metals may produce a catalyst whose behaviour may differ from that of catalysts prepared by traditional methods [3–6]. On the other hand, CuCo catalysts have been studied extensively, especially related to their performance in the CO hydrogenation reaction [7,8]. Taking into account these considerations, we now report the preparation and study of a new CuCo silica-supported catalyst. The heterogeneization of a

* Corresponding author. Tel.: +34-934021235; Fax: +34-934907725; E-mail: nhoms@kripto.qui.ub.es
[1] Also corresponding author.

1381-1169/99/$ - see front matter
PII: S1381-1169(99)00179-X

bimetallic Cu–Co organometallic complex has been carried out. An H_2 treatment of the solid at low temperature led to the catalyst, which has been characterized by X-ray diffraction (XRD), transmission electron microscopy (TEM), energy-dispersive X-ray analysis (EDX), electron microdiffraction, X-ray photoelectron spectroscopy (XPS) and Fourier Transform Infrared Spectroscopy (FTIR). Very small silica-supported Co particles, some of which interact with copper aggregates were obtained. The structural characteristics of the catalyst have been related to its catalytic behaviour in ethylene hydroformylation and CO hydrogenation reactions.

2. Experimental

2.1. Catalyst preparation

The support used was Degussa Aerosil-type silica with a BET surface area of 200 $m^2\ g^{-1}$. Previous to the catalyst preparation, SiO_2 was partially dehydroxylated by treatment under high vacuum at 473 K for 16 h. Then the support (SiO_2 200) was impregnated with a methylene chloride solution of the complex [Cu(TMDE)Co-$(CO)_4$], prepared following methods described in the literature [9]. After impregnation, the solid was washed with methylene chloride, and then treated under high vacuum (10^{-5} mbar) at room temperature for 6 h and further left in contact with CO (200 mbar) at 373 K overnight. The resulting solid was then carefully reduced under H_2 at 473 K for 6 h.

The cobalt and copper content of the catalyst was determined by atomic absorption spectroscopy: Cu 2.39% (wt/wt); Co 2.08% (wt/wt).

2.2. Characterization methods

For the infrared measurements the sample was prepared 'in situ' in a special greaseless cell, which allowed high vacuum-gases and thermal treatments.

Adsorption of a CH_2Cl_2 solution of the metallic precursor onto a previously partially dehydroxylated SiO_2 wafer (SiO_2 200) was carried out in the strict absence of oxygen and water using break-seal techniques. Infrared spectra were recorded on a Nicolet 520 Fourier transform spectrophotometer working with a resolution of 2 cm^{-1}.

XRD pattern of powder was collected at a step width of 0.02° and by counting 10 s at each step in the range of interest using a Siemens D-500 X-ray diffractometer equipped with a graphite monochromator and a Cu target.

TEM combined with EDX was carried out on a Hitachi H 800-MT electron microscope working at 150 kV equipped with a Kevex analytical system. The X-rays emitted upon electron irradiation were acquired in the range 0–10 keV. Samples were supported on carbon-coated titanium grids by depositing a drop of the specimen suspended in methanol.

Photoelectron spectra (XPS) were acquired with a VG Escalab 200 R spectrometer equipped with a hemispherical electron analyzer and MgKα ($h\nu = 1254.6$ eV) X-ray source, powered at 120 W. The powder sample was pressed into small aluminum supports and then mounted on a support rod placed in the pretreatment chamber. Prior to being moved into the analysis chamber the sample was exposed to H_2 at 473 K for 1 h. Peak intensities were estimated by calculating the integral of each peak after smoothing and substraction of the S-shaped background and fitting the experimental curve by a least squares routine using Gaussian and Lorentzian lines. Atomic ratios were computed from the intensity ratios normalized by atomic sensitivity factors [10]. The binding energy (BE) reference was taken at the Si 2p peak at 103.4 eV. An estimated error of 0.1 eV can be assumed for measurements.

2.3. Catalytic activity

Carbon monoxide hydrogenation was carried out under continuous flow (30 ml min^{-1}) and

differential conditions at a total pressure of 50 bar between 433 and 473 K with a H_2:CO = 2:1 molar ratio. The reaction products were analyzed on-line by gas chromatography.

Hydroformylation of ethylene was carried out in an 80-ml magnetically stirred stainless-steel autoclave at a total pressure of 76 bar and 453 K with a C_2H_4:CO:H_2 1:1:1 molar ratio. After the reaction time, the reaction products were collected in toluene maintained at 194.5 K and analyzed by gas chromatography and mass spectrometry, using a GC-MS Hewlett-Packard apparatus with a 5971 mass-selective detector.

3. Results and discussion

3.1. Interaction of Cu–Co complex with the silica support

The impregnation step was followed 'in situ' by FTIR as indicated in Section 2. Spectrum (a) in Fig. 1 corresponds to the sample obtained after impregnation of [Cu(TMDE)Co(CO)$_4$] onto a wafer of SiO_2(200) and a subsequent treatment under high vacuum at room temperature. In Fig. 1, the spectrum of the impregnating solution is also shown (spectrum (b)). A comparison of both spectra ((a) and (b) in Fig. 1) indicates that, after impregnation, the ν(CO) pattern of the surface species is similar to that of the complex even if it is not so well-resolved and bands now appear at slightly higher wavenumbers. On the other hand, the FTIR spectrum corresponding to the ν(OH) region showed a decrease in the band appearing at 3745 cm^{-1}, corresponding to isolated silanol groups, and the appearance of a broad shoulder at lower wavenumbers ca. 3646 cm^{-1}, characteristic of silanol group H-bonding. The hydrogen bonding of the complex may be favoured through the bridging CO, which is the more basic carbonyl oxygen in the precursor.

Treatment of the resulting sample with CO up to 348 K produced a somewhat different ν(CO) pattern, in which the band at lower wavenumbers ca. 1845 cm^{-1} (Fig. 2, spectra (a), (b)) was not seen. The band of silanol groups remain unchanged during this treatment. In these conditions, the cleavage of the Cu-(bridging CO) bond may occur.

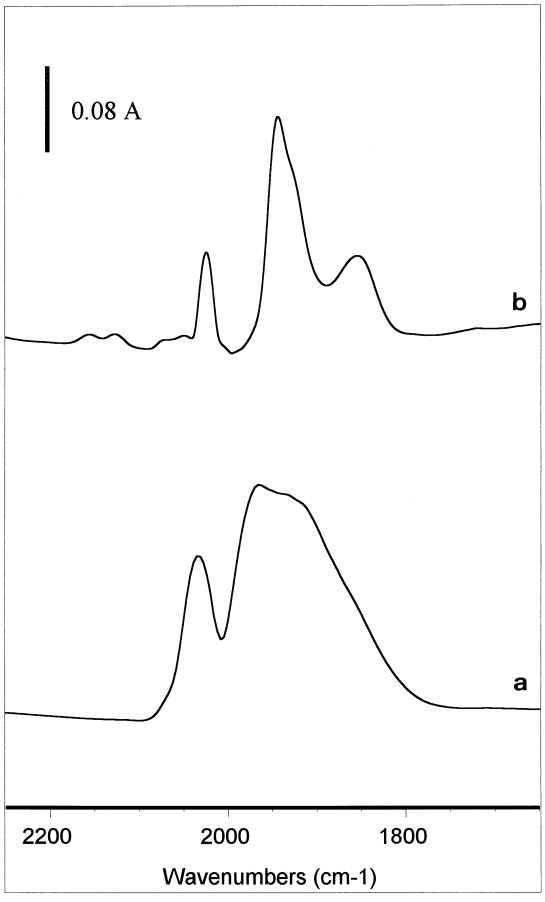

Fig. 1. (a) Infrared spectrum of SiO_2(200) after impregnation with a methylene chloride solution of [Cu(TMDE)Co(CO)$_4$], and subsequent high vacuum treatment. (b) Infrared spectrum of [Cu(TMDE)Co(CO)$_4$] impregnating solution.

The initial surface species transformed clearly upon treatment under CO up to 373 K, as deduced from inspection of Fig. 2. Moreover, the ν(OH) intensity of isolated silanol groups was recovered. The ν(CO) bands due to the initial surface species disappeared after the CO treatment at 373 K. Simultaneously, the progressive formation of a band at ca. 1896 cm^{-1} can be observed (Fig. 2, spectra (a–c)). This band was clearly visible after this CO treatment

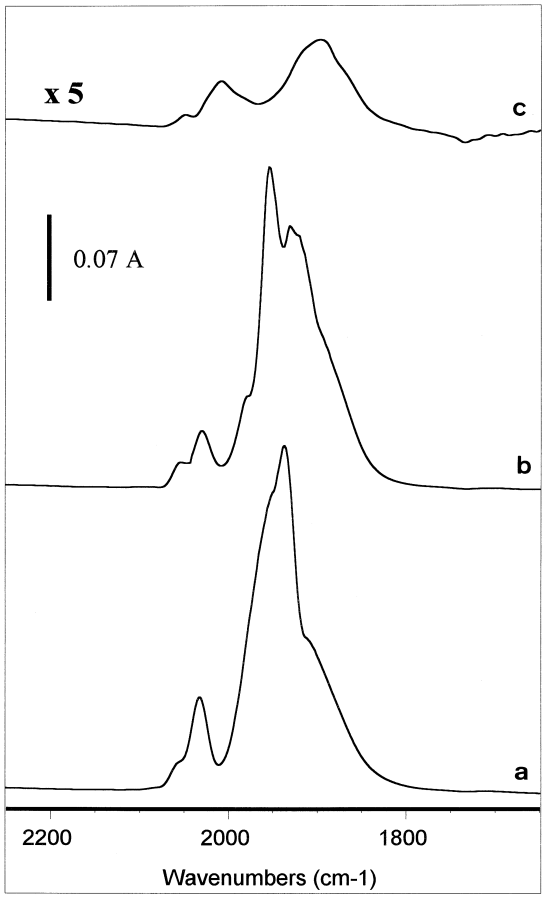

Fig. 2. Infrared spectra in the ν(CO) region of the initial species treated under 50 mbar of CO from 298 to 373 K. (a) After treatment at 298 K. (b) After spectrum (a) treatment at 348 K. (c) After spectrum (b) treatment at 373 K.

at 373 K and a subsequent vacuum treatment at 298 K (Fig. 3, spectrum (a)). This rather broad band centered at 1896 cm^{-1} may be assigned to $[Co(CO)_4]^-$ in a slightly distorted Td environment [11–13]. The formation of this $[Co(CO)_4]^-$ is related to the breakdown of the Co–Cu bond on the initial surface species.

The increase in temperature up to 373 K under vacuum produced the total decarbonylation of this species (Fig. 3, spectrum (b)). A new CO treatment at 473 K produced spectrum (c) in Fig. 3. No bands assigned to carbonyl cobalt species are present, but a new band with maximum at 2079 cm^{-1} appears, which presents high asymmetry on the higher wavenumber values, and can be deconvoluted into three components, with maxima at 2122, 2099 and 2078 cm^{-1} (Fig. 3, spectrum (d)). The component at 2099 cm^{-1} can be assigned to CO over Cu(0) [14]. On the other hand, that at higher wavenumber, 2122 cm^{-1}, may arise from CO over partially oxidized Cu [14], even if CO over Co-interacting Cu may also lead to the observation of a band at this position [15,16]. The main component at 2078 cm^{-1} may correspond to CO over very small particles of Co(0) [17] or even Co-carbonylic species on the support. Indeed, when $Co_2(CO)_8$ interacts with silica, an easy evolution to $Co_4(CO)_{12}$ was reported, this

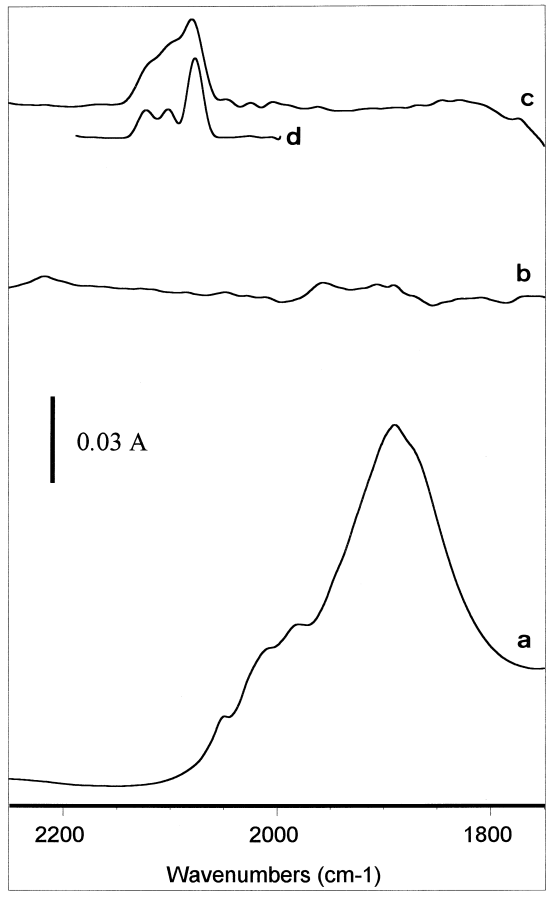

Fig. 3. Infrared spectra in the ν(CO) region. (a) Initial species after a CO treatment at 373 K and subsequent vacuum treatment at 298 K. (b) After spectrum (a) vacuum treatment at 373 K. (c) After spectrum (b) sample was treated with CO (50 mbar) at 373 K. (d) Mathematical deconvolution of spectrum (c).

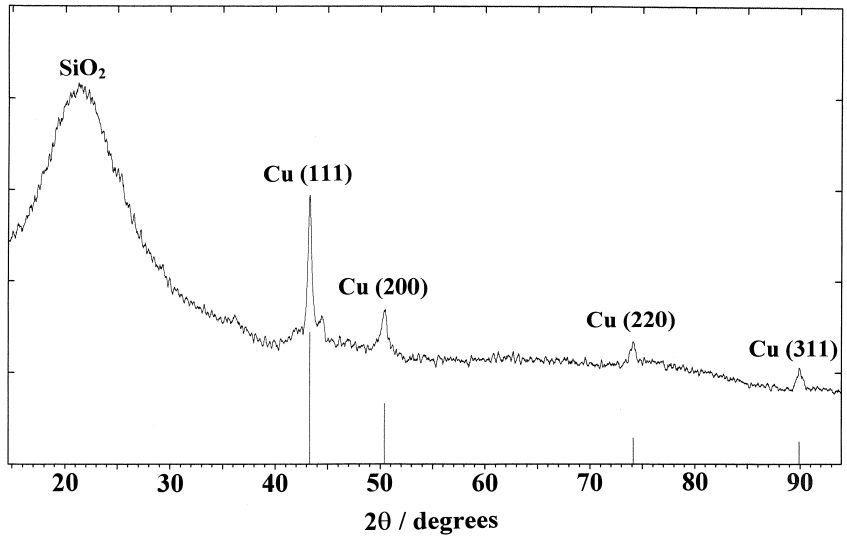

Fig. 4. XRD pattern of the $CuCo/SiO_2$ catalyst.

species on silica shows a main band at 2072 cm^{-1} [12]. On the other hand, $Co_4(CO)_{12}$ was shown to be stable on silica under CO up to 473 K [18].

3.2. Catalyst characterization

After the hydrogen treatment at 473 K, the catalyst was characterized by different techniques. XRD analysis of the catalyst gave the diffraction pattern shown in Fig. 4. Only peaks corresponding to the presence of Cu metallic particles are present.

Fig. 5 shows a representative bright-field micrograph of the catalyst obtained by TEM. Large metallic aggregates constituted by smaller individual crystallites are visible. All EDX performed on these metallic aggregates indicated the common occurrence of both Cu and Co. Furthermore, in all cases, the Cu K lines were much more intense than the Co K lines, indicating that the metallic aggregates are enriched in copper with respect to the initial Cu:Co = 1:1 precursor ratio. For example, one of these EDX patterns is shown in Fig. 6(A). Electron diffraction microanalysis were carried out on some of these particles. Fig. 7 shows one of them. The diffraction pattern contains both spots and rings. The diffraction spots correspond to a copper particle oriented along the crystallographic [111] direction, whereas the diffraction rings correspond to the main reflections of multiple, much smaller cobalt particles. When other regions of the catalyst were analyzed by EDX, cobalt was detected and no Cu was detected in any case. Indeed, during ED and EDX measurements, the formation of metallic Co particles was probably induced by the electron irradiation. Fig. 6(B) shows a representative EDX analysis carried out on the support.

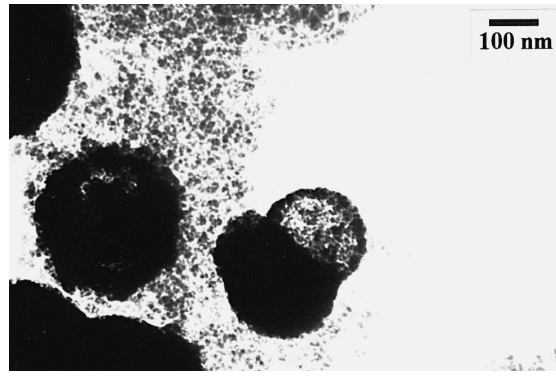

Fig. 5. Representative TEM micrograph of the $CuCo/SiO_2$ catalyst.

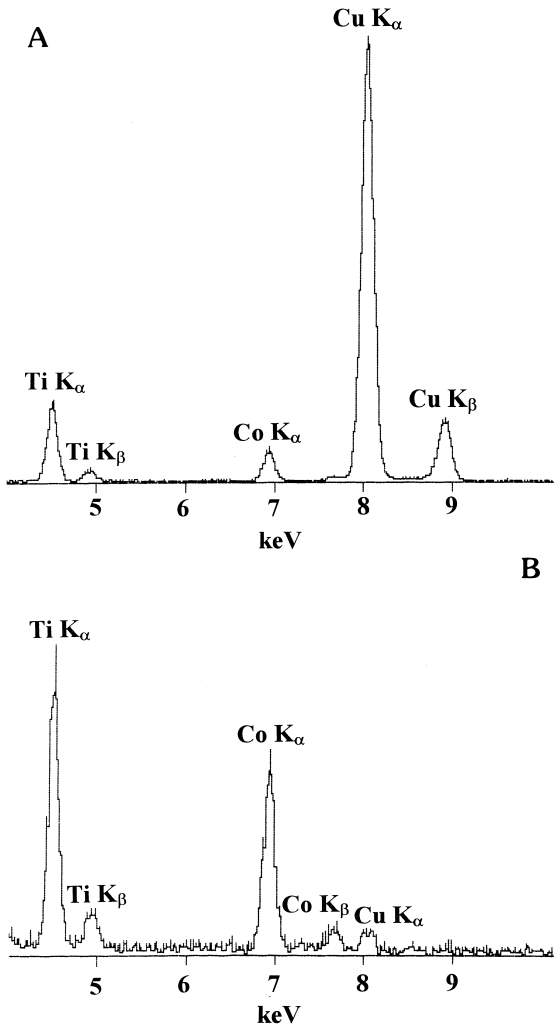

Fig. 6. (A) EDX pattern of representative particle of the $CuCo/SiO_2$ catalyst. (B) EDX pattern obtained when analysis was performed on the support.

The energy regions of Si 2p, N 1s, Cu $2p_{3/2}$ and Co $2p_{3/2}$ core levels were recorded. The respective BEs are compiled in Table 1, and the computed surface atomic ratios are summarized in Table 2. The weak N 1s peak observed at a BE of 399.8 eV may be related to the presence of remaining ligand, which was not fully removed during the hydrogen treatment. The BE of Cu $2p_{3/2}$ level appears in the same energy region of bulk metallic copper, which is consistent with the observation of large copper particles by XRD. On the other hand, although the

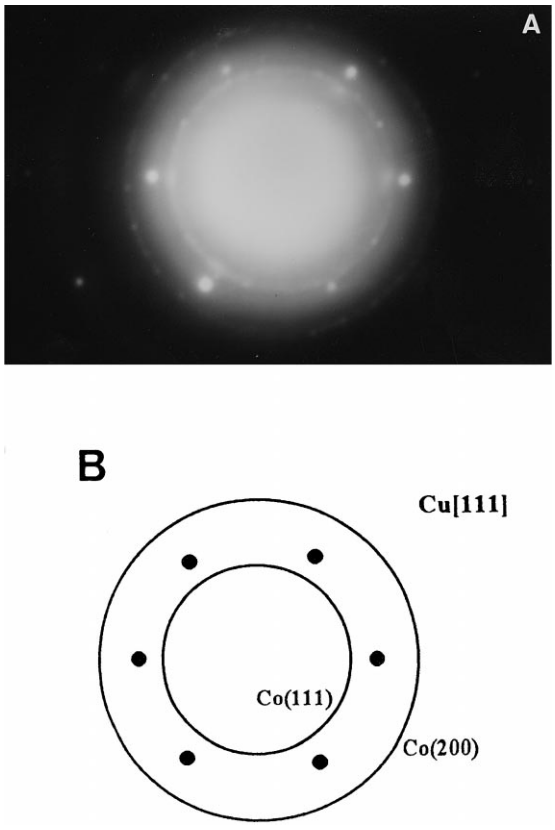

Fig. 7. (A) Electron microdiffraction pattern of a representative particle of the $CuCo/SiO_2$ catalyst. (B) Indexed pattern shown in (A).

Co $2p_{3/2}$ line profile is more complex, its position indicates that only oxidized cobalt is detected by XPS. The appearance of a small component at 782.6 eV indicates the formation of very small cobalt oxide particles. The observation of a satellite component in the peak profile is conclusive that cobalt remains as Co^{2+}. The surface Cu/Co atomic ratio computed from the peak intensity ratio (Cu/Co = 0.074) is conclu-

Table 1
BE (eV) of core electrons of the atoms for the $CuCo/SiO_2$ catalyst reduced at 473 K

Si 2p	N 1s	Cu $2p_{3/2}$	Co $2p_{3/2}$
103.4	399.8	932.0	782.6 (10) 784.8 (90)[a]

Number in parentheses are peak percentages.
[a] Peak area also includes satellite line.

Table 2
Surface atomic ratios of reduced catalyst

$(N/Si)_{atom}$	$(Cu/Si)_{atom}$	$(Co/Si)_{atom}$	$(Cu/Co)_{atom}$
0.003	0.028	0.378	0.074

sive that Co dispersion was very much higher than that of copper, in agreement with results derived from XRD and TEM measurements.

An IR study of CO coordination after catalyst reduction was also carried out. The catalyst was reduced under H_2 at 473 K, and then treated under high vacuum at the same temperature. The catalyst was then exposed to 50 mbar of CO at room temperature. The FTIR spectrum obtained in the ν(CO) region is shown in Fig. 8. A broad band appeared at 2081 cm^{-1}, which

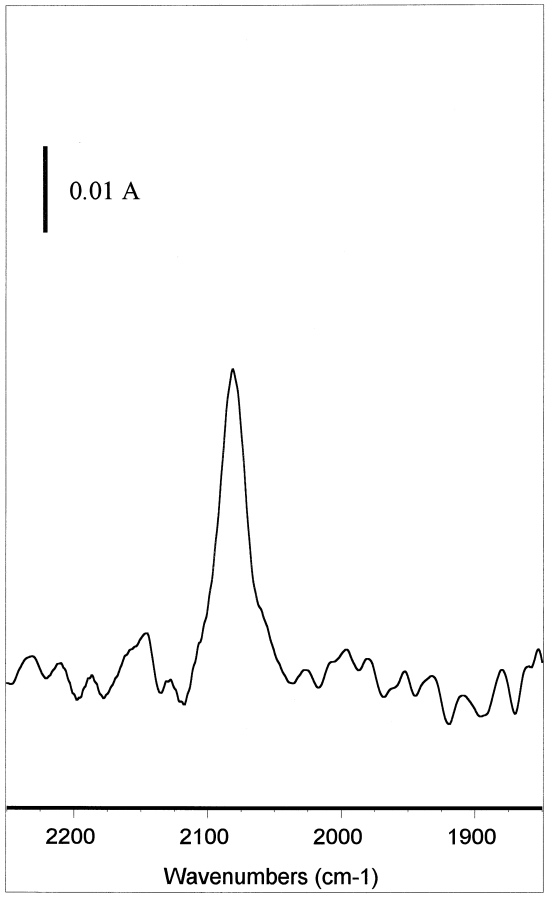

Fig. 8. Infrared spectrum in the ν(CO) region of reduced catalyst treated with CO (50 mbar) at 473 K.

Table 3
CO hydrogenation reaction over the $CuCo/SiO_2$ catalyst[a]

T (K)	CO conv. (%)	Selectivity (%)			
		C1	C2+	MeOH	C2+OH
433	2.4	36	21	32	11
453	1.9	35	22	32	11
473	1.5	30	36	26	8

[a]Reaction conditions: P_{total}: 50 bar, $H_2/CO = 2/1$, catalyst charge: 0.25 g, reactant flow = 30 ml min^{-1}.

remained after CO treatment at 373 K. The position of this band is coincident with that of the component at lower wavenumber obtained before the hydrogen treatment (Fig. 3, spectrum (c)) which was assigned to CO over very small particles of Co(0) or even to Co-carbonylic species on the support.

The presence of copper aggregates interacting or not with highly dispersed cobalt is proposed from all the characterization data discussed above.

3.3. Catalytic activity

The results on the CO hydrogenation reaction are reported in Table 3. The catalytic study was carried out at increasing temperatures from 433 to 473 K. All catalytic data were taken after 2 h at a given temperature. The slightly lower CO conversion values obtained when temperature was increased may be due to the catalyst stability under reaction conditions. Under the experimental conditions used, hydrocarbons and alcohols were produced (approx. 60% hydrocarbons, 40% alcohols). Not only methanol, but also ethanol and propanol were produced (32%

Table 4
Ethylene hydroformylation reaction over the $CuCo/SiO_2$ catalyst[a]

CO conv. (%)	Selectivity (%)		
	C_2H_5CHO	C_3H_7OH	$(C_2H_5)_2CO$
4.3	73.9	2.4	23.7

[a]Reaction conditions: P_{total}: 76 bar, $T = 453$ K, $C_2H_4/CO/H_2 = 1/1/1$, catalyst charge: 1 g, reaction time 24 h.

MeOH, 11% EtOH + PrOH). The production of higher alcohols indicates that the migratory CO insertion into a metal–alkyl bond is favoured over this catalyst. Taking into account that this is a common step to the hydroformylation reaction [19], the ethylene hydroformylation was also tested over the $CuCo/SiO_2$ catalyst. The results obtained are summarized in Table 4. Propanal, propanol, and 3-pentanone were obtained; the formation of propanol and 3-pentanone was attributed, respectively, to the subsequent hydrogenation or condensation of propanal, which is the primary product of the ethylene hydroformylation. The remarkable selectivity of the $CuCo/SiO_2$ catalyst towards higher alcohols in the CO hydrogenation reaction and its behaviour in the hydroformylation reaction may be related to the presence of highly dispersed cobalt interacting with copper aggregates.

Acknowledgements

We thank DGICYT (MAT96-0859-C02-01) and Generalitat de Catalunya (1995SGR 00285) for financial support.

References

[1] I. Yu, B. Yermakov, N. Kuznetsov, V.A. Zakharov (Eds.), Catalysis by Supported Complexes, Stud. Surf. Sci. and Catal., 8, Elsevier, 1981.
[2] R. Whyman, in: J.-M. Basset et al. (Eds.), Surface Organometallic Chemistry: Molecular Approaches to Surface Catalysis, Vol. 231, NATO, Serie C, Kluwer Academic Publishers, 1986, p. 75.
[3] J. Zwart, R. Snel, J. Mol. Catal. 30 (1985) 305.
[4] A. Trunschke, H. Ewald, H. Miessner, A. Fukuoka, M. Ichikawa, H.-C. Böttcher, Mater. Chem. Phys. 29 (1991) 503.
[5] F.S. Xiao, A. Fukuoka, M. Ichikawa, J. Catal. 138 (1992) 206.
[6] L. Huang, Y. Xu, Catal. Lett. 40 (1996) 203.
[7] P. Courty, D. Durand, E. Freund, A. Sugier, J. Mol. Catal. 17 (1982) 241.
[8] J.P. Hindermann, G.J. Hutchings, A. Kiennemann, Catal. Rev.-Sci. Eng. 35 (1993) 1.
[9] G. Doyle, K.A. Eriksen, D. Van Engen, Organometallics 4 (1985) 877.
[10] D. Briggs, M.P. Seah, in: Practical Surface Analysis. Auger and X-Ray Photoelectron Spectroscopy, 2nd edn., Wiley, Chichester, 1990.
[11] W. Hieber, Adv. Organomet. Chem. 8 (1970) 1.
[12] R. Schneider, R.F. Howe, K.L. Watters, Inorg. Chem. 23 (1984) 4593.
[13] N. Homs, A. Choplin, P. Ramírez de la Piscina, L. Huang, E. Garbowski, R. Sánchez-Delgado, A. Théolier, J.-M. Basset, Inorg. Chem. 27 (1988) 4030.
[14] N. Sheppard, T.T. Nguyen, in: Advances in Infrared and Raman Spectroscopy, Vol. 5, Chap. 2, 1978, and references therein.
[15] R.M. Bailliard Letournel, A.J. Gomez-Cobo, C. Mirodatos, M. Primet, J.A. Dalmon, Catal. Lett. 2 (1989) 149.
[16] A. Gomez-Cobo, N. Mouaddib, J.A. Dalmon, C. Mirodatos, V. Perrichon, M. Primet, P. Chaumette, Ph. Courty, in: A. Holmen et al. (Eds.), Natural Gas Conversion, Elsevier, Amsterdam, 1991, p. 257.
[17] J. Llorca, N. Homs, J. Sales, P. Ramírez de la Piscina, J. Mol. Catal. A 96 (1995) 49.
[18] J. Kiviaho, M.K. Niemelä, Y. Morioka, K. Kataja, Appl. Catal. 144 (1996) 93.
[19] J. Llorca, A. Barbier, G.A. Martin, J. Sales, P. Ramírez de la Piscina, N. Homs, Catal. Lett. 42 (1996) 87.